Ocean Surface Current Measurement with an Interferometric UHF SAR

Mark Sletten, *IEEE Senior Member*, Steven Menk, *IEEE Member*, Jakov Toporkov, *IEEE Senior Member*

***Abstract*—In this paper, we report initial results of an experimental investigation into measurement of ocean surface currents with an ultra high frequency synthetic aperture radar (UHF SAR) that supports an along-track interferometric (ATI) mode. We first describe the unique system, the NRL Multiband SAR, used to collect the data. We then present initial results related to two different approaches to current measurement. In the first approach, the surface current is estimated using standard ATI-SAR processing. We show progress in the implementation of this method with an interferometric phase cut across the north wall of the Gulf Stream. In the second, a time-sequence of images of propagating wave-like patterns is first generated using sub-aperture processing of the wide-beam, strip-map data, and this sequence is then transformed into wavenumber-frequency space through a 3D FFT. The surface current is then estimated from the displacement of the wave energy relative to the theoretical surface wave dispersion relation in the absence of any underlying current. We illustrate our progress in this approach with a wavenumber-frequency analysis of a 41-second sub-aperture image sequence of propagating waves.**

***Index Terms*—ATI-SAR, ocean current measurement**

I. INTRODUCTION

For three decades, along-track interferometric synthetic aperture radar (ATI-SAR) has been under development as a sensor for the measurement of ocean surface currents. From the earliest single-beam experiments, through the development of vector, dual-beam systems as well as in recent space-borne implementations, SAR systems operating in the microwave band above 1 GHz have been used [1, 2, 3]. This frequency choice was driven primarily by the desire for high spatial resolution coupled with practical limits on antenna size and along-track spacing. However, the higher microwave band poses a challenge when it comes to extracting the true surface *current* from the ATI-SAR measurement of the surface *velocity.* Due to the influence of transient capillary waves in the microwave band and their modulation by longer ocean waves, it can be difficult to accurately model and then remove the wave-induced component of the measured velocity in order to determine the underlying current.

The UHF band promises to alleviate this problem while also opening up new approaches to surface current measurement. In the UHF band, the fundamental radar scatterering centers are longer-lived, hydrodynamically linear surface waves with wavelengths on the order of 1 m, as opposed to transient capillaries, thereby simplifying the required scattering model. But in addition, the wide azimuthal beamwidth of a typical UHF SAR supports a second, completely independent approach to current measurement. Through sub-aperture processing of the wide-beam data, a time sequence of wave-like images can be produced that contains information on any underlying currents that may be present. As described below, currents alter the dispersion relation between the wavelength and propagation speed of the surface waves, and the image time-sequence provided by sub-aperture processing promises to provide a means to measure this alteration. This “wave dispersion” approach has been used effectively with *land-based, real-aperture* radar systems as well as with optical systems to measure both currents as well as bathymetry [4, 5], but attempts to implement it with a SAR though sub-aperture processing have not yet been reported in the literature. In this paper, we present initial results from an experimental investigation designed to explore these potential UHF SAR advantages.

II. THE NRL MBSAR

The data analyzed in this investigation were collected using the Naval Research Laboratory Multiband SAR (NRL MBSAR), a flexible, multi-channel system that operates in both the UHF and L bands simultaneously. The system supports an instantaneous UHF bandwidth as high as 700 MHz (200-900 MHz), but due to spectrum management considerations, UHF data are usually collected in multiple sub-bands. Transmit waveforms are completely programmable and two transmit channels are available for each band through the use of high-power switches. The acquisition system supports 6 simultaneous receive channels at a digitization rate of 2.3 GS/s. In the lowest RF sub-band (230-290 MHz), the antenna has an azimuthal beamwidth approaching 80 degrees. At a typical aircraft altitude of 5000 ft, ground speed of 120 m/s, and slant range of 3 km, any point in the beam can be imaged for approximately 40 s.

For the present study, the system was configured on a P3 Orion aircraft to operate in dual-band, polarimetric, interferometric modes. Dual-polarized UHF antennas were installed in both the nose and tail to support polarimetric along-track interferometry, while a single, dual-polarized L-band antenna was installed in the tail. All antennas were boresited broadside to the aircraft at an incidence angle of 60 degrees. UHF data were collected in polarimetric-interferometric modes with baselines of 14.5 and 29 m. The nominal ground speed of

The authors are with the US Naval Research Laboratory, Washington DC 20375 USA (e-mail: mark.sletten@ nrl.navy.mil).

the aircraft was 120 m/s, producing interferometric lags of 0.12 and 0.24 s.

III. Ocean Current Measurement Methods

A. Traditional ATI-SAR

Using the traditional ATI-SAR method, the radial component of the surface current is derived from the interferometric phase, ψ_{AT} , between two images, I_{fore} and I_{aft}, generated by two phase centers separated along the flight direction. This phase difference is generated by scene motion that occurs during the effective time delay between the two images, and is thus proportional to the total radial surface velocity, u_r,

$$u_r = \frac{\psi_{AT}\lambda}{4\pi B_{eff}} V_p \quad (1)$$

Here B_{eff} is the effective spacing between the antennas in the flight direction, V_p is the aircraft ground speed, and λ is the radar wavelength. ψ_{AT} is the phase of the interferogram between the two images.

Note that u_r is not the actual underlying surface current, u_c. It is the sum of that current plus a velocity component generated by wave motion, u_{wave}, i.e., $u_r = u_c + u_{wave}$. Removal of u_{wave} to determine u_c is normally accomplished by subtraction of an estimate of u_{wave} generated by a model. At microwave frequencies above 1 GHz, this modeling step can be challenging due to the dependence on transient wind-driven capillary waves and their modulation by longer waves as well as hydrodynamically nonlinear breaking waves. In contrast, the Bragg-scattering paradigm for ocean scattering assumes that UHF backscatter is generated by longer-lived, longer wavelength, linear water waves, and thus models are expected to be simpler and more accurate. One of the objectives of our investigation is to determine if this makes UHF SAR the preferred sensor for measuring ocean currents for some applications and under some conditions.

.

B. Wave Dispersion

Current estimation through wave dispersion is based upon the observed relationship between the spatial wavenumber of the surface waves, $\boldsymbol{k_w}$, and their temporal frequency at any point in space, ω. In the presence of a current, $\boldsymbol{U}$, and assuming linear waves in deep water, basic hydrodynamic analysis leads to the following expression for this relationship

$$(\omega - \boldsymbol{k}_w \cdot \boldsymbol{U})^2 = g|\boldsymbol{k}_w| \quad (2)$$

where g is the acceleration due to gravity. (Note that $\boldsymbol{k}_w$ and $\boldsymbol{U}$ are vectors.) Solving this expression for the radial component of the current leads to

$$|\boldsymbol{U}| cos\theta = \frac{\omega - \sqrt{g|\boldsymbol{k_w}|}}{|\boldsymbol{k_w}|} \qquad (3)$$

where θ is the angle between the current and wave propagation directions.

In order to measure ω and $\boldsymbol{k_w}$ and then estimate the current from (3), we exploit the long aperture produced by the wide azimuthal beamwidth of a UHF SAR to generate a *time sequence* of images. We segment the data into sub-apertures and form an image from each one to form a time-stack of images (a "movie") over the long interval of time during which any point in the scene stays in the wide UHF SAR antenna beam. This interval exceeds 40 seconds for the data shown below, and it allows observation of wave propagation. A 3D FFT of this time-stack transforms the data into a 3D space in which the frequency and wavenumber of these patterns, ω_{SAR} and $\boldsymbol{k_{wSAR}}$, can be determined. Assuming $\omega_{SAR} \cong \omega$ and $\boldsymbol{k_{wSAR}} \cong \boldsymbol{k_w}$, (3) can then be used to determine the current. However, wave motion has long been known to cause distortion in SAR ocean imagery, so this assumption cannot necessarily be made. An objective of our research is to characterize distortion in the $\omega - k$ domain and investigate strategies to mitigate it.

IV. Experimental Results

Data were collected in support of this investigation in 2017 and 2018 off the Atlantic coast of North Carolina over a wind speed range of 2-15 m/s and for significant wave heights as high as 13 ft. Flight tracks were selected to emphasize the strong current signatures provided by the north wall of the Gulf Stream (GS), located (cloud cover permitting) via AVHRR satellite imagery before each flight.

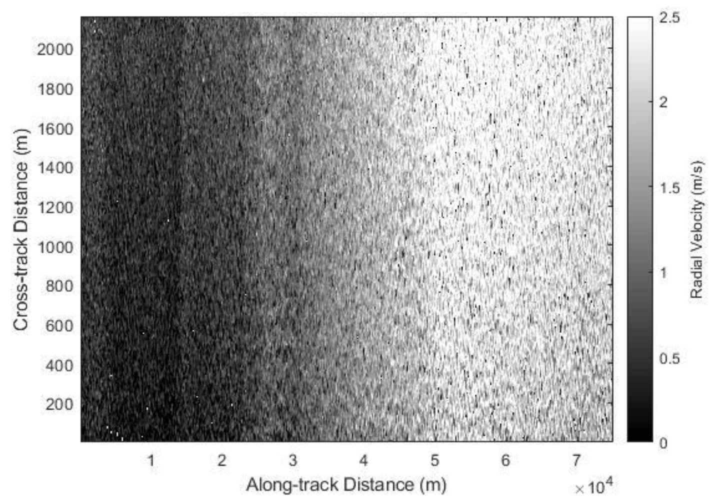

Fig. 1 Along-track interferometric velocity generated from images collected over the north wall of the Gulf Stream

Fig. 1 shows a UHF (230-290 MHz) interferogram generated from images collected over a long pass centered on the probable location of the GS north wall on July 31, 2017. The radar look direction was towards the northeast, roughly parallel to the expected Gulf Stream flow direction, as the aircraft flew southeast at an altitude of 5000 ft. A steady increase in the radial velocity towards the northeast can be observed along with several small step increases. Coherent averaging of the interferogram over the entire range dimension produces the velocity profile plotted in Fig. 2, which shows a

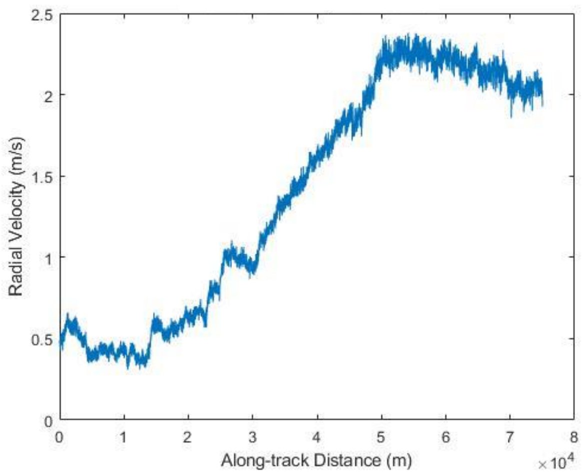

Fig. 2 Velocity cut across the north wall of the Gulf Stream, obtained through coherent averaging across the cross-track (range) direction of the interferogram of Fig. 1

total increase in velocity of approximately 1.8 m/s. This increase in speed across the velocity front is comparable to the typical peak Gulf Stream velocity of 2.5 m/s. Note that the *change* in interferometric velocity across the front is a good estimate of the *change* in surface current, since the (as yet) unknown value of u_{wave} is expected to be essentially constant. The images were vertically polarized. The velocity scale was determined from (1) using the baseline of 14.5 m, the aircraft velocity of 126 m/s, and an RF wavelength of 1.15 m, corresponding to the center of the image's 230-290 MHz sub-band. The velocity reference for the data in both Figs 1 and 2 was determined using other imagery containing (stationary) land. Positive velocities correspond to flow away from the SAR.

Progress in our investigation of the dispersion method can be seen Figs. 3 and 4. Fig. 3 contains a single sub-aperture velocity image from a 41-second sequence that displays clearly defined propagating wave patterns. (A movie of the entire sequence will be included in the conference presentation.) The quantity displayed is the phase of the interferogram formed by the nose and tail sub-aperture images, rather than the magnitude of either image, as we have found that the wave patterns are more visible in the phase. The wave patterns propagate nearly in the range direction, towards the radar (i.e. towards the southwest), in general agreement with directional wave spectra available from NDBC buoy 44014 located approximately 40 km to the northwest. A sub-aperture time of 7 seconds was selected to generate the images in the sequence, based upon a qualitative assessment of the wave pattern contrast. A slice through the peak of the corresponding $\omega - k$ spectrum is shown in Fig. 4, along with the theoretical dispersion curve computed from (2) assuming $|\boldsymbol{U}| = 0$. The observed spectrum occupies a narrow region of $\omega - k$ space near the dispersion curve, with a peak located at $\omega_{SAR} = 0.61$ rad/s and $|\boldsymbol{k_{wSAR}}| = 0.044\ \mathrm{m}^{-1}$. From (3), this indicates a surface current of 1.1 m/s towards the NE, in reasonable agreement with the traditional ATI-SAR current values plotted in Fig. 2. In the conference presentation, we will present the results of repeated application of this

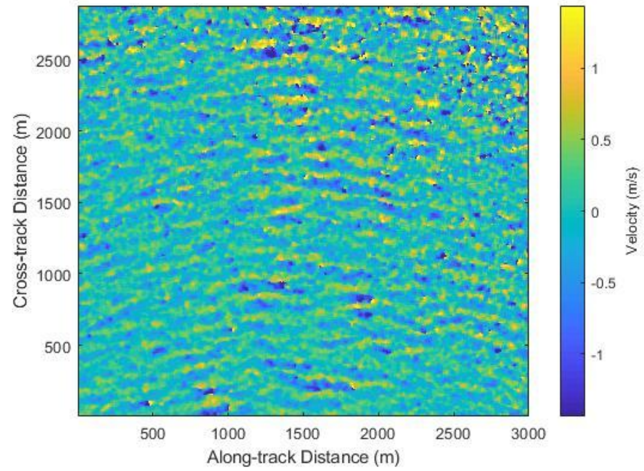

Fig. 3 Example velocity image taken from a 41-second image sequence produced by sub-aperture processing of the long MBSAR aperture.

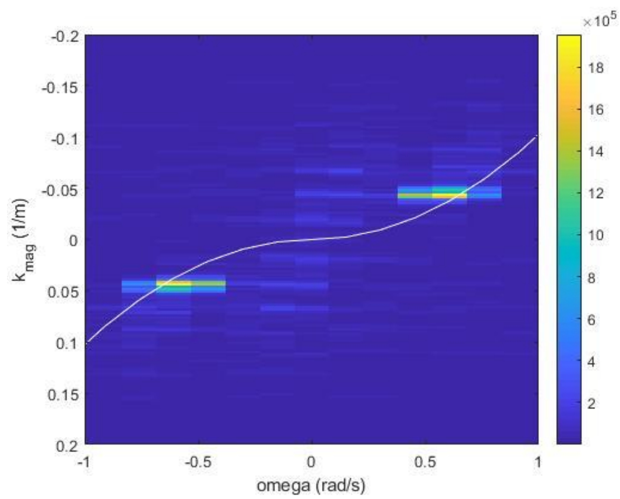

Fig. 4 Color-coded data: Slice through the peak of the wavenumber-frequency spectrum generated by a 3D FFT of a 41-second sub-aperture image sequence. White line: Theoretical dispersion relation

analysis along the flight track to determine how well the trend matches that shown in Fig. 2.

V. SUMMARY

In this paper, we present initial results of an experimental investigation into UHF ATI-SAR as a sensor for the measurement of ocean surface currents. This investigation covers two measurement approaches: standard ATI-SAR processing in which the current is derived from the interferometric phase, and a wave dispersion method that uses a time sequence of sub-aperture images to infer the relationship between the spatial wavenumber of the waves and their propagation velocity. Our initial results include reasonable agreement between currents implied by a first-ever UHF ATI-SAR interferogram over the north wall of the Gulf Stream and by a wavenumber-frequency analysis of an image sequence of propagating, wave-like patterns.

REFERENCES

[1] Goldstein, R. M., and H. A. Zebker, "Interferometric radar measurement of ocean surface currents", *Nature*, Vol 328, August 1987

[2] Toporkov, J. et al, "Sea Surface Velocity Vector Retrieval Using Dual-Beam Interferometry: First Demonstration", *IEEE Trans on Geosci Remote Sensing*, Vol. 43, No. 11, November 2005

[3] Romeiser, R. et al, "First Analysis of TerraSAR-X Along-Track InSAR-Derived Current Fields", *IEEE Transactions on Geoscience and Remote Sensing*, Vol. 48, No. 2, February 2010

[4] Frasier, S and R. McIntosh, "Observed wavenumber-frequency properties of microwave backscatter from the ocean surface at near-grazing angles", J. Geophysical Research, Vol. 101, No. C8, Aug. 1996

[5] Dugan, J. et al, "Near-Surface Current Profile Measurements Using Time Series Optical Imagery", *Proceedings of the IEEE/OES/CMTC Ninth Working Conference on Current Measurement Technology*, Charlston SC, USA, March 2008